

1 Utilizing random regression models for genomic prediction of a longitudinal
2 trait derived from high-throughput phenotyping

3 Malachy Campbell^{1,2}, Harkamal Walia¹, and Gota Morota²

4 ¹Department of Agronomy and Horticulture, University of Nebraska Lincoln

5 ²Department of Animal Science, University of Nebraska Lincoln

6 **Corresponding author:**

7 Malachy Campbell

8 Department of Animal Science, Department of Agronomy and Horticulture

9 University of Nebraska Lincoln

10 Lincoln, Nebraska 68583

11 Email: campbell.malachy@gmail.com

12 Abstract

13 The accessibility of high-throughput phenotyping platforms in both the greenhouse and field,
14 as well as the relatively low cost of unmanned aerial vehicles, have provided researchers with
15 an effective means to characterize large populations throughout the growing season. These
16 longitudinal phenotypes can provide important insight into plant development and responses
17 to the environment. Despite the growing use of these new phenotyping approaches in plant
18 breeding, the use of genomic prediction models for longitudinal phenotypes is limited in
19 major crop species. The objective of this study is to demonstrate the utility of random
20 regression (RR) models using Legendre polynomials for genomic prediction of shoot growth
21 trajectories in rice (*Oryza sativa*). An estimate of shoot biomass, projected shoot area
22 (PSA), was recored over a period of 20 days for a panel of 357 diverse rice accessions using
23 an image-based greenhouse phenotyping platform. A RR that included a fixed second-order
24 Legendre polynomial, a random second-order Legendre polynomial for the additive genetic
25 effect, a first-order Legendre polynomial for the environmental effect, and heterogeneous
26 residual variances was used to model PSA trajectories. The utility of the RR model over
27 a single time point (TP) approach, where PSA is fit at each time point independently, is
28 shown through four prediction scenarios. In the first scenario, the RR and TP approaches
29 were used to predict PSA for a set of lines lacking phenotypic data. The RR approach showed
30 a 11.6% increase in prediction accuracy over the TP approach. Much of this improvement
31 could be attributed to the greater additive genetic variance captured by the RR approach.
32 The remaining scenarios focused forecasting future phenotypes using a subset of early time
33 points for known lines with phenotypic data, as well new lines lacking phenotypic data. In all
34 cases, PSA could be predicted with high accuracy (r : 0.79 to 0.89 and 0.55 to 0.58 for known
35 and unknown lines, respectively). This study provides the first application of RR models for
36 genomic prediction of a longitudinal trait in rice, and demonstrates that RR models can be

37 effectively used to improve the accuracy of genomic prediction for complex traits compared
38 to a TP approach.

Keywords: Genomic prediction, high-throughput phenotyping, phenomics, genetics

1 Introduction

With the advent of next-generation sequencing technologies, the biology community has experienced a rapid increase in the amount of genotypic data that is available. These developments, along with the low cost of sequencing, has encouraged the adoption of genomic selection (GS) approaches in plant breeding. With these approaches, genome-wide SNP markers are used to estimate an individuals additive genetic contribution to a given trait, and genotyped individuals can be selected and advanced to further generations without phenotypic evaluation (Meuwissen et al., 2001; Jannink et al., 2010; Endelman, 2011). Although these approaches have increased genetic gain through the acceleration of breeding cycles, considerable resources must still be devoted to the accurate phenotypic evaluation of individuals (Furbank and Tester, 2011). This necessary step remains a major bottleneck for many breeding programs.

In recent years, considerable investment, in both the public and private sector, have been made to automate the phenotypic characterization of large populations. Large investments have been made to build high-throughput phenotyping facilities in both the greenhouse and field where highly controlled water, nutrient, or temperature regimes can be applied to individual plots, and plants can be routinely monitored throughout the development using imaging. Moreover, the relatively low cost of drones that can be fitted with cameras and other sensors, have provided researchers with an effective means to characterize large populations throughout the growing season (Furbank and Tester, 2011; Chapman et al., 2014; Zhang et al., 2016; Watanabe et al., 2017). These longitudinal phenotypes can provide important insight into the mechanisms that underlie physiological responses to environmental stresses and developmental processes, and can be leveraged to improve prediction accuracies for complex polygenic traits, such as yield that have been a target for most breeding programs (Fahlgren et al., 2015; Campbell et al., 2017; Sun et al., 2017). Despite the growing use of

65 these new phenotyping approaches in plant breeding, the use of models for genomic selection
66 (GS) for longitudinal phenotypes is limited in breeding major crop species. Most conventional
67 field studies involve one or a few evaluations throughout the growing season, thus repeated
68 phenotypic measurements on the same plant or plot is relatively rare.

69 Several approaches have been utilized for GS using longitudinal data. A simple repeata-
70 bility (SR) model was used by Sun et al. (2017) and Rutkoski et al. (2016) for secondary
71 longitudinal traits. The SR model treats each time point as a repeated measure of the same
72 trait and assumes that the variance for all records are equal and the correlation between
73 time points is constant. However, for many traits recorded across many time points, the
74 assumption behind SR model is not realistic. A multivariate approach can be extended
75 to longitudinal data. However, the computational complexity of the multivariate approach
76 increases with the number of time points, and becomes unfeasible with high frequency lon-
77 gitudinal traits due to the large number of parameters to estimate. Often, the number of
78 observations necessary to accurately estimate parameters exceeds the size of most studies.

79 Random regression (RR) models have proven to be an attractive alternative to the above
80 methods, and have been utilized in livestock and tree breeding (Apiolaza et al., 2000; Bermejo
81 et al., 2003; Nobre et al., 2003; Bohmanova et al., 2008; Costa et al., 2008; Wetten et al., 2012;
82 Howard et al., 2015). Here, covariance functions are explicitly defined that are equivalent
83 to the full covariance matrix of the trait across time points (Kirkpatrick et al., 1990; Meyer,
84 1998). Covariance functions include, but are not limited to banded correlation, autoregressive
85 models, orthogonal polynomials, or spline functions (Meyer, 1998; Apiolaza et al., 2000).
86 Thus, these models utilize a few parameters to describe the full covariance, and are much
87 more computationally efficient. In animal breeding, RR models have been used extensively
88 to estimate hertiabilities and perform pedigree-based prediction of important longitudinal
89 traits such as growth, feed intake, fat, and milk production (Bermejo et al., 2003; Nobre
90 et al., 2003; Bohmanova et al., 2008; Costa et al., 2008; Wetten et al., 2012; Howard et al.,

91 2015).

92 The increased accessibility to high-throughput phenotyping platforms provides the plant
93 science community with high frequency temporal measurements for complex polygenic phe-
94 notypes. These data are very different from those typically used for genomic prediction in
95 which phenotypes are recorded at a single time point or at harvest for large populations.
96 However, the availability of these new data presents an opportunity to extend these ap-
97 proaches used extensively for longitudinal traits in animal breeding to major crops. Here,
98 we demonstrate the use of RR models to predict shoot growth trajectories in a rice diversity
99 panel. Specifically, the aims of this study are to (1) examine the advantage of utilizing
100 longitudinal phenotypes over single end-point measurements (cross-sectional GS), (2) de-
101 termine whether longitudinal phenotypes collected during early time-points can be used to
102 predict phenotypes at later time points (i.e. forecasting lines with records), and (3) predict
103 future phenotypes for new lines using early records for existing lines.

104 **2 Materials and Methods**

105 **2.1 Plant materials and greenhouse conditions**

106 Three hundred seventy eight lines of the Rice Diversity Panel 1 were selected for this study
107 (Zhao et al., 2011). Seed propagation is described in Campbell et al. (2015). Three uniformly
108 germinated seedlings were selected and transplanted to pots (150mm diameter x 200 mm
109 height) filled with approximately 2.5 kg of UC Mix (the actual weight varied from experiment
110 to experiment by 100-200 g). Square containers were placed below each pot to allow water
111 to collect.

112 2.2 Experimental Design

113 All experiments were conducted at the Plant Accelerator, Australian Plant Phenomics Fa-
114 cility, at the University of Adelaide, SA, Australia. Each experiment consisted of 378 lines
115 and was repeated three times from February to April 2016. Two smarthouses were used
116 for each experiment, with 216 pots positioned across 24 lanes in each smarthouse. Each
117 experiment consisted of a partially replicated design, with 54 randomly selected lines having
118 two replicates in each experiment.

119 Seven days after transplant (DAT), plants were thinned to one seedling per pot. Two
120 layers of blue mesh was placed on top of the pots to reduce soil water evaporation. The
121 plants were loaded on the imaging system and were watered to 90% field capacity at 11
122 DAT.

123 2.3 Image analysis

124 The plants were imaged daily from 13 to 33 DAT using a visible (red–green–blue camera;
125 Basler Pilot piA2400–12 gc, Ahrensburg, Germany) from two side-view angles separated
126 by 90° and a single top view. The three experiments produced a total of 72,537 images.
127 "Plant pixels" were extracted from RGB images using the LemnaGrid software. Briefly,
128 plant pixels were extracted from background objects using a color classification strategy.
129 Two set of colors were chosen manually to represent plant and background objects. For
130 each image, pixels were assigned as background or plant pixels using the nearest-neighbor
131 method. For a given pixel, this method assigns the pixel to a predefined color by finding
132 the most similar (smallest Euclidean distance) color in the set. Noise (i.e. small areas of
133 non-plant pixels) in the image is removed using a series of erosion and dilation steps.

134 The sum of the "plant pixels" from the three RGB images were summed, and used as a
135 measure of shoot biomass. Here this trait is referred to as projected shoot area (PSA). This

metric has been shown to be an accurate representation of shoot biomass (Campbell et al., 2015; Goltzarian et al., 2011; Knecht et al., 2016). Prior to downstream analyses, outlier plants at each time point were detected for each trait using the 1.5(IQR) rule. Plants that were flagged as potential outliers were plotted and inspected visually. Those that exhibited abnormal growth patterns were removed. A total of 32 plants were removed, leaving a total of 2,604 plants for downstream analyses.

2.4 Selection of random regression models

PSA was modeled across all twenty time points using several RR models. Following the notation of Mrode (2014), the RR models can be summarized as

$$\text{PSA}_{tjk} = \mu + \sum_{k=0}^2 \phi(t)_{jk} \beta_k + \sum_{k=0}^{nr} \phi(t)_{jk} u_{jk} + \sum_{k=0}^{nr} \phi(t)_{jk} s_{jk} + e_{tjk} \quad (1)$$

Here β is the fixed second-order Legendre polynomial to model the overall trend in the trait overtime, u_{jk} and s_{jk} are the k^{th} random regression coefficients for additive genetic effect and random experiment of line j , nr is the order of polynomial for the random effects, and e_{tjk} is the random residual. The order of β was selected based on visual inspection of the trends. Various polynomial functions and residual variance structures were evaluated for line and experiment, and residuals, respectively. A complete description of the models is provided in Table 1. For each trait, the models were ranked based on goodness-of-prediction using Akaike's information criterion (AIC) scores (Akaike, 1974).

2.5 Genomic selection at each time point

A mixed model approach was used to fit genomic best linear unbiased predictions (gBLUPs) at each time point using the following model.

$$\mathbf{y} = \mathbf{Z}\mathbf{u} + \mathbf{Q}\mathbf{s} + \mathbf{e}, \quad (2)$$

Here, \mathbf{y} is the PSA at time t ; \mathbf{Z} and \mathbf{Q} are incidence matrices corresponding to the random additive genetic effect (\mathbf{u}), and random experimental effect (\mathbf{s}), respectively; and \mathbf{e} is the random residual error. The variances were based on the following assumptions $\mathbf{u} \sim N(0, \mathbf{G}\sigma_g^2)$, $\mathbf{s} \sim N(0, \mathbf{I}\sigma_s^2)$, and $\mathbf{e} \sim N(0, \mathbf{I}\sigma_e^2)$. Here, σ_g^2 is the additive genetic variance; σ_s^2 is an environmental variance associated with experiment; and σ_e^2 is the residual variance. A genomic relationship matrix (\mathbf{G}) was calculated using VanRaden (2008).

$$\mathbf{G} = \frac{\mathbf{Z}_{\text{cs}}\mathbf{Z}_{\text{cs}}'}{m} \quad (3)$$

156 Here, \mathbf{Z}_{cs} is a centered and scaled $n \times m$ matrix, where m is 33,674 SNPs and n is the 357
157 genotyped rice lines.

158 2.6 Genomic selection using random regression

159 For each trait, the "best" random regression model was used to predict gBLUPs. The
160 following mixed model was used to predict gBLUPs

$$\text{PSA}_{tjk} = \mu + \sum_{k=0}^2 \phi(t)_{jk}\beta_k + \sum_{k=0}^2 \phi(t)_{jk}u_{jk} + \sum_{k=0}^1 \phi(t)_{jk}s_{jk} + e_{tjk} \quad (4)$$

161 The variables are the same as in *Selection of random regression models*, however note that nr
162 has been replaced with 2 and 1 for the additive genetic and experiment effect, respectively.
163 Thus the random additive genetic effects are described using a second-order Legendre poly-
164 nomial, while a first-order Legendre polynomial is used to describe the experiment effects

165 across time points.

In matrix notation, the model is

$$\mathbf{y} = \mathbf{Z}\mathbf{u} + \mathbf{Q}\mathbf{s} + \mathbf{e}, \quad (5)$$

166 with all vectors and matrices defined as above. However here u is now a vector of random
167 regression coefficients for the additive genetic effects. The variances were based on the
168 following assumptions $\mathbf{u} \sim N(0, \mathbf{G} \otimes \mathbf{\Omega})$, $\mathbf{s} \sim N(0, \mathbf{I} \otimes \mathbf{P})$, and $\mathbf{e} \sim N(0, \mathbf{I} \otimes \mathbf{D})$. Here, $\mathbf{\Omega}$
169 is a 3×3 covariance matrix of random regression coefficients for additive genetic effects; \mathbf{P}
170 is a 2×2 covariance matrix of random regression coefficients for experiment effect; and \mathbf{D}
171 is a diagonal matrix allowing for heterogeneous variances over time points. \mathbf{Z} and \mathbf{Q} are
172 covariable matrices where the i th row contains the orthogonal polynomials for the i th day
173 of imaging. Thus, matrix \mathbf{Z} is the covariable matrix for the additive genetic effects with a
174 dimension of $t \times nk$ where nk is the order of Legendre polynomial for the additive genetic
175 effect multiplied by the number of individuals with phenotypic records and t refers to the
176 number of days of imaging. Similarly, \mathbf{Z} is a $t \times ns$ covariable matrix for the experiment
177 effect, where ns is the the order of the Legendre polynomial for the experiment effect (e.g. 1)
178 time the number of experiments (e.g. 3). Variance components and gBLUPs were obtained
179 using ASREML (Release 4.0) (Gilmour et al., 2015).

180 Using the method above, variance components were obtained for additive genetic and
181 environmental components. For the additive genetic term, each line has three random re-
182 gression coefficients ($nr = 0, 1, 2$). gBLUPs were predicted at each time point according to
183 Mrode (2014). For a given line, j , at time t the gBLUPs can be obtained by $\text{gBLUP}_{jt} = \phi_t \hat{u}_j$;
184 where ϕ_t is the row vector of the matrix of Legendre polynomials of order 2.

2.7 Estimation of narrow-sense heritability

To estimate the narrow sense heritability, variance components were obtained for each random term using ASREML for the TP analyses and the RR approach. For the RR approach, additive genetic variance was obtained at each time points using methods described by Mrode (2014). Briefly, for time i the genetic variance can be obtained by $\mathbf{t}_i\mathbf{\Omega}\mathbf{t}'_i$, where $\mathbf{t}_i = \phi_{ik}$, the i th row vector of the matrix of Legendre polynomials at different time points (ϕ) for the i th day of imaging, $\mathbf{\Omega}$ is the covariance matrix of RR coefficients for the genetic effects, and k is the order of fit. The variance of the experimental effect across time points was calculated using the same approach. For both the single time point analysis h^2 was estimated as

$$\frac{\sigma_g^2}{\sigma_s^2 + \sigma_s^2 + \sigma_e^2}.$$

2.8 GS scenarios and cross validation

Four scenarios were tested using GS (Figure 1). In the first scenario (scenario A), all twenty time points were used to fit a RR model and phenotypes were predicted for a set of lines without phenotypic records. The second scenario (scenario B), the dataset was split into two datasets each consisting of ten consecutive time points. A RR model was fitted using the first ten time points and was used to predict the phenotypes for the same set of lines in the last ten time points. Scenario C, can be thought of as a combination of scenarios A and B. Here, the dataset was split into four subsets, with each quadrant consisting of 178 to 179 lines and ten time points. Here, a RR model was fitted using ten early time points for half the lines with known phenotypes, and was used to predict the phenotypes in the last ten time points for the remaining 178 to 179 lines. Finally, in the last scenario (Scenario D) we sought to predict the shoot biomass at a later time points in an independent study. This can be thought of as forecasting for new lines in an independent study. A publicly available dataset was used in which 359 lines (357 lines in common between the two studies) were

209 phenotyped from 20 to 40 days after transplant, thus a 13 day overlap was available for the
210 two datasets, and a RR model was fitted using phenotypic information from the time points
211 in the first experiment for 179 lines, and was used to predict gBLUPs for the remaining 178
212 lines in a second independent experiment described by Campbell et al. (2017).

213 To assess the accuracy of gBLUPs for the TP GS as well as scenarios A, C, and D, a
214 two-fold cross validation approach was used. Briefly, the 357 lines were split into two sets,
215 with one serving as a training set with known phenotypes and the second serving as a testing
216 set with unknown phenotypes. Since the number of lines were not even the remaining line
217 was assigned to the training set. The accuracy of prediction was assessed by comparing
218 predicted gBLUPs with observed PSA at each of the three experiments using Pearson's
219 correlation method. The lines were randomly assigned to each fold, and the process was
220 repeated 20 times. For each fold, the average correlation over the three experiments was
221 used, and the average over the two folds was used for each resampling run. For scenario B,
222 half of the lines were randomly selected and the first ten time points were used to predict the
223 phenotypes in the last ten time points for the same lines. Again, the variance in prediction
224 accuracy was assessed by randomly sampling half the lines for analysis. Pearson's correlation
225 was computed for the gBLUPs and PSA as described above.

226 **3 Results**

227 A rice diversity panel was phenotyped over a period of twenty days during the early vegetative
228 stage using an automated high-throughput phenotyping platform. The panel consists of 357
229 lines from 80 countries, and captures much of the genetic diversity within cultivated rice
230 (Zhao et al., 2011).

231 The plants were imaged each day using RGB cameras from three angles (two side view
232 angles separated by 90 degrees and one top view). The plant pixels from each image were

233 summed and used to estimate shoot biomass. Here, this metric is referred to as PSA and
234 has been shown to be an accurate measure of shoot biomass in cereals (Berger et al., 2010;
235 Campbell et al., 2015). This experiments captures the early vegetative stage of development,
236 where shoot biomass increases nearly exponentially (Figure 2).

237 **3.1 Random regression model selection**

238 RR models have been used extensively to model longitudinal phenotypes in animal breeding.
239 These models are particularly advantageous in that differences in the shape of the curve
240 can be accounted for, and can be solved using the conventional mixed model framework.
241 Thus, in the scope of genetics, these models allow for inter-individual variation in the mean
242 trend to be estimated. Here, the overall mean growth trend was modeled using a second-
243 order Legendre polynomial. A total of eight models were evaluated to identify a model
244 that adequately described the data and could be used for GS. Each model included a fixed
245 second-order Legendre polynomial to describe the overall mean growth trend, while several
246 Legendre polynomials ranging from zero to second-order Legendre polynomials were fitted
247 for random genetic and experimental effects. The residual effects were assumed to be constant
248 or heterogeneous across time points using an identity or diagonal matrix, respectively. The
249 "best" model was selected based on the smallest AIC value. Table 1 provides an overall
250 summary of the models and the corresponding AIC values. The "best" model (Model 8) was
251 one that included a fixed second-order polynomial to model the mean trend in shoot growth,
252 a second-order Legendre polynomial for the random additive genetic effect, a first-order
253 Legendre polynomial for the experimental effect, and the residual variance was assumed to
254 be heterogeneous over time points.

3.2 Genetic correlation and narrow sense heritability of PSA

To examine the relationship for PSA between time points, the phenotypic and genetic correlation was estimated. Estimates for the overall phenotypic correlations were high (r : 0.49 - 1.0), with the highest correlation observed between adjacent time points (Figure 3A). The genetic correlation followed a similar pattern, with an overall high correlation (r : 0.84 - 1.0) observed among pairwise comparisons of all 20 time points. As above, adjacent time points exhibited the highest genetic correlation ($r = 1$), while those further apart exhibited lower correlation (Figure 3B). Interestingly, a strong genetic correlation was observed between day 1 and day 20 ($r = 0.91$), indicating that shoot growth (e.g. PSA) may be driven by similar genetic mechanisms at the early seedling and active tillering stage in rice.

To evaluate the ability of the longitudinal RR approach to capture additive genetic variance, the narrow sense heritability of PSA was estimated using the RR model described above and a conventional mixed model at each time point. The mixed model included random terms for the additive genetic and experimental effect. For both models, a genomic relationship matrix was generated using 33,674 markers for the 357 lines. On average, the RR approach showed a 44% increase in the heritability of PSA compared to the TP approach (Figure 4). The TP approach showed a mean h^2 of 0.50 over all time points, while the RR approach showed an h^2 of 0.71 on average. h^2 ranged from 0.60 to 0.77 for the RR approach, while h^2 ranged from 0.46 to 0.57 for the TP approach. The two approaches showed nearly identical h^2 estimates on day 1, however at later time points h^2 of RR was considerably higher than TP. These results suggest that the RR approach captures more additive genetic variance for PSA than the TP approach.

3.2.1 Utility of longitudinal phenotypes for genomic prediction

The availability of high throughput phenotyping platforms provides a means to accurately phenotype large populations for a number of traits throughout time. While phenotypes

280 recorded at a high frequency over time will likely improve the accuracy of GS, few reports
281 have demonstrated the advantages of longitudinal phenotypes in major crops or model plant
282 systems. Here, the utility of longitudinal phenotypes for GS was evaluated under four hypo-
283 theoretical scenarios (Figure 1). The first scenario can be thought of as a standard GS approach
284 (Figure 1A). Here, all 20 time points for half of the 357 lines used to predict the phenotypes
285 at all 20 time points for the remaining lines. The aim of scenario A is to determine whether
286 the longitudinal RR approach provides greater prediction accuracy than a cross-sectional
287 GS approach in which a mixed model is fit at each time point. The first training set can be
288 thought of as existing lines with phenotypic records and the test population as a new set of
289 lines without records. The aim of scenario B (Figure 1B), is to determine if traits at later
290 time points can be predicted for known lines using information at early time points. Thus, it
291 can be considered as a forecasting approach. Here, longitudinal phenotypes are available for
292 lines during the early time points (1-10 days of imaging), and are used to predict phenotypes
293 for the same lines at later time points. Scenario C (Figure 1C), can also be considered a
294 forecasting approach however for new lines. Here a subset of lines with phenotypes during
295 the first 10 time points are used to predict the phenotypes for new lines without phenotypes
296 at the later time points. In scenario D (Figure 1D), we sought to predict the shoot biomass
297 at a later time points in an independent study. Here, a publicly available dataset was used
298 in which 359 lines (357 lines in common between the two studies) were phenotyped from 20
299 to 40 days after transplant, thus a 13 day overlap was available for the two datasets. A RR
300 model was fitted using phenotypic information from the time points in the first experiment
301 for 179 lines, and was used to predict gBLUPs for the remaining 178 lines in the second
302 experiment.

303 **Scenario A: Comparison between longitudinal RR and cross-sectional GS**

304 To evaluate the advantages of using the longitudinal phenotype for PSA for GS over a single
305 time points, the prediction accuracy of the RR model described above was compared to a
306 conventional cross-sectional approach in which the additive genetic effects were estimated
307 at each time point. For both approaches, two-fold cross validation was performed in which
308 half the lines were randomly selected as a training set, and the remaining half was used for
309 prediction. Pearson’s correlation was used to assess the accuracy between predicted gBLUPs
310 and observed PSA in the test set for each experiment. The average correlation across all
311 three experiments was determined for each fold. The resampling process was repeated ten
312 times.

313 Overall, the RR model showed significantly higher prediction accuracies than the TP
314 approach (Figure 5A). On average, the longitudinal phenotype improved prediction accuracy
315 by 11.6% (mean across all time points) compared to the TP approach. The prediction accu-
316 racies for the TP approach ranged from 0.40 to 0.60, while for the RR approach accuracies
317 ranged from 0.47 to 0.58. Although the TP approach exhibited low prediction accuracies
318 during the early time points and increasing prediction accuracies toward the end of the study,
319 the prediction accuracy for the RR model remained relatively constant with a slight increase
320 in r observed from day 1 to 9. The largest improvements in prediction accuracy was observed
321 between 5 to 10 days of imaging, with the RR model showing 35% higher accuracy at day
322 8 compared to the TP approach. Collectively, these results indicate that RR models can be
323 used to improve the accuracy of genomic prediction for longitudinal phenotypes.

324 **Scenario B: Forecasting existing lines**

325 Here, the the objective is to predict future phenotypes for lines with phenotypic trajectories
326 recorded earlier in the growing season or development. To this end, the dataset was separated
327 into two, with the first ten time points serving as a training set to predict the phenotypes

328 for the last ten days. This approach is described in Figure 1B. The RR model described
329 above was fit to the data. To assess the accuracy of prediction, two-fold cross validation was
330 performed in which 50% of the lines were randomly selected for training and prediction, and
331 the resampling process was repeated ten times. The accuracy of prediction was very high,
332 ranging from 0.79 to 0.82 for the last ten time points without phenotypic records (Figure
333 5B). A slight decline in prediction accuracy was observed after day 10, with day 11 exhibiting
334 the highest accuracy ($r = 0.82$) and the lowest accuracy on day 20 ($r = 0.79$). This trend in
335 prediction accuracy is expected, given that the phenotypic records at day 11 should be very
336 highly correlated with those at day 10, with the correlation declining as time progresses.
337 The high predictive ability observed indicates that the first ten time points is sufficient to
338 accurately predict future phenotypes for known lines.

339 **Scenario C: Forecasting new lines**

340 As shown above, future phenotypes can be accurately predicted from longitudinal traits at
341 early time points for existing lines. While the knowledge of performance of known lines at fu-
342 ture time points may be beneficial in some applications, GS is most often used to select lines
343 without prior knowledge of the phenotype. Previously in scenario A, we showed that pheno-
344 types could be predicted accurately for new lines using the complete longitudinal phenotype.
345 Here, the aim is to predict future phenotypes for new lines with no phenotypic records using
346 early phenotypic records for existing lines. To this end, the dataset was partitioned into
347 two temporal datasets, with the first ten time points serving as a training set to predict the
348 phenotypes for the last ten days (Figure 1C). As above, a two-fold cross validation approach
349 was used to assess prediction accuracy. Half the lines were randomly assigned to each fold,
350 and the first ten time points from the first fold were used to predict the phenotypes at the
351 last ten time points in the second fold. The prediction accuracies for scenario B were very
352 similar to those observed for scenario A. Accuracies ranged from 0.48 to 0.57, with the pre-

353 diction accuracy ranging from 0.55 to 0.57 in the last ten days (Figure 5C). The prediction
354 accuracies showed a slight increase from day 1 to day 9. The highest prediction accuracy
355 was observed at day 15, while the lowest accuracy was observed at day 1. These results
356 suggest that future phenotypes can be forecast for new lines with reasonable accuracy using
357 phenotypic records from earlier time points for a set of known lines.

358 **Scenario D: Forecasting new lines at later time points in an independent study**

359 In scenario C, we have shown that gBLUPs for new lines can be accurately predicted using
360 phenotypes for a set of known lines at a subset of early time points. Here, the objective
361 was to expand this approach and evaluate the utility of the RR model to predict gBLUPs
362 for new lines at future time points in an independent study. Here, we utilized an existing
363 dataset where 359 lines from the rice diversity panell were phenotyped from 20 to 40 days
364 after transplant (Figure 1D.). Although there is overlap between developmental stages of
365 this dataset and the dataset used for scenarios A-C, this experiment was conducted at a
366 different time of year and therefore the photoperiod and light intensity should be different
367 between the two.

368 A RR model was fitted that was identical to that used for scenarios A-C, in that it
369 included a fixed second-order polynomial to model the mean trend in PSA, a second-order
370 Legendre polynomial for the random additive genetic effect, a first-order Legendre polynomial
371 for the random experimental effect, and a heterogeneous residual variance over time points.
372 The RR model was fitted using phenotypes for 179 lines from the early vegetative stage
373 experiment (i.e. 13 to 32 DAT), and the genetic values for the RR coefficients were used to
374 predict the phenotypes for the remaining 178 lines in the second experiment (i.e. 20 to 40
375 DAT). A two-fold cross validation approach was used in which phenotypes across all twenty
376 days were selected for 179 lines in the first experiment and were used to predict gBLUPs for
377 the remaining 178 lines in the second experiment.

378 The prediction accuracy was high with r values ranging from 0.51 to 0.59 (Figure 5D).
379 The prediction accuracy was relatively constant, but showed a slight increase in accuracy
380 from 22 to 29 days after transplant. An increase in the prediction accuracy was observed
381 from 13 to 31 DAT, after which the prediction accuracy declined slightly. The second time
382 point (22 DAT) exhibited the lowest prediction accuracy ($r = 0.51$). The highest prediction
383 accuracy was observed on day 34 after transplant ($r = 0.59$). Collectively, these results
384 suggest that longitudinal phenotypes can be accurately predicted in an independent study
385 using the RR approach.

386 **3.3 Discussion**

387 High-throughput phenotyping platforms provide an accessible means to record traits non-
388 destructively for large populations throughout development. Such longitudinal data provide
389 an opportunity to understand the genetics of the development of a phenotype, and identify
390 individuals that exhibit desirable trait trajectories. However, such data provides new chal-
391 lenges to adapt approaches utilized for single time point phenotypes in plant genomics and
392 breeding to accommodate longitudinal data. This study provides the first application of RR
393 models for genomic prediction of a longitudinal trait in rice.

394 **Advantages of RR over univariate genomic prediction**

395 The predictive ability in GS is dependent on the heritability of the trait, the number of
396 markers, population size, linkage disequilibrium (LD), and the number of QTL influencing
397 the trait (Daetwyler et al., 2008, 2010). Here, the RR model using longitudinal phenotypes
398 provided greater prediction accuracy compared to a TP gBLUP. The predictive ability of
399 the RR approach improved prediction accuracies by 11.6% on average compared to TP
400 analysis. The number of markers, population size, LD, and the number of QTL influencing
401 PSA are held constant between the two models. Thus, the difference in prediction accuracy

402 hold be largely attributed to the differences in heritability between the RR approach and
403 TP analysis. As shown in Figure 4, the RR approach accounted for more additive genetic
404 variance than the TP analysis. Similar gains in heritability for height in Swedish Scots pine
405 has been reported by Wang et al. (2009) with RR models that utilize B-splines or Legendre
406 polynomials over TP analyses. Moreover, when the prediction accuracy is expressed as
407 the ratio of the correlation of gBLUPs and observed PSA to the square root of h^2 , both
408 approaches were nearly equivalent (Figure 6). Thus, the higher prediction accuracy is due
409 to the higher h^2 of the RR approach relative to the TP approach.

410 With both methods (RR and TP), we observed high prediction accuracies ranging from
411 0.4 - 0.6 (Arruda et al., 2015; Duhnen et al., 2017; Kristensen et al., 2018; Leplat et al.,
412 2016). While similar accuracies have been reported by other studies for complex traits,
413 it is important to note that the current study utilized a diversity panel with considerable
414 population stratification and the prediction models did not account for population structure.
415 Accounting for population structure is important in genome wide association studies to
416 reduce spurious associations (Yu et al., 2006). However, these corrections can often hinder
417 the ability to detect true QTL that are correlated with population structure (Zhao et al.,
418 2011). With GS, the aim is to achieve high prediction accuracies across subpopulations rather
419 than to detect QTL associated with the trait (Hayes et al., 2009; Lorenz et al., 2011). Thus,
420 the high prediction accuracies observed for the models used in this study may be due, in
421 part, to population structure, and the random sampling of individuals across subpopulations
422 during CV should reduce the possibility of having a training set that is strongly imbalanced
423 by a given subpopulation.

424 **Utilizing RR prediction for forecasting phenotypes**

425 The utilization of genomic information to predict future outcomes is not new. Considerable
426 effort in the field of personalized medicine has been devoted to predict disease risks for in-

427 individuals based on genomic information. Here, disease-associated loci are used to predict
428 potential future outcomes for individuals (Moser et al., 2015). The ability to predict future
429 phenotypes using phenotypic information collected early in the life cycle may be advanta-
430 geous in plants, particularly perennial species with long life cycles. Selection during the early
431 developmental stage can shorten evaluation times.

432 Here, we evaluated the ability of RR models to predict future phenotypes using pheno-
433 typic records collected during the early time points. This was performed for known lines
434 (e.g. those with early records; Scenario B), as well as new lines (Scenario C and D). We
435 observed high prediction accuracies for each forecasting scenario. As expected the highest
436 accuracy was observed for Scenario B, in which early phenotypic records are used to predict
437 future phenotypes for the same set of lines. Surprisingly, high prediction accuracies were
438 also observed when early records for known lines were used to predict future phenotypes
439 for unknown lines (Scenarios C and D). In both cases, the accuracies were not significantly
440 different from those achieved when using phenotypic information for all time points. These
441 results collectively indicate that the future phenotypes can be accurately predicted using a
442 subset of the temporal phenotypes. While these results are encouraging, these forecasting
443 approaches will be highly dependent on the temporal genetic architecture of the trait. The
444 lack of decline by utilizing only a subset of time points is likely due to the high genetic cor-
445 relation observed between time points. The similar genetic architecture between the early
446 and late time points that is evidenced by the strong positive genetic correlation (Figure 3B)
447 estimated between early (1-10 days) and late (11-20 days) time points. Thus, we suggest
448 to first evaluate the genetic correlation between time points for the trait of interest before
449 utilizing such forecasting approaches.

450 3.4 Conclusion

451 High throughput phenomics platforms have provided the plant science community with a
452 means to generate high resolution temporal phenotypes for large populations at a relatively
453 low cost. RR models that utilize Legendre polynomials provide a flexible for genomic pre-
454 diction of longitudinal traits. These approaches provide several advantages over single time
455 point analyses: (1) these models account for more additive genetic variance compared to
456 the TP analysis, which translates to higher predictive accuracies; (2) future phenotypes can
457 be accurately predicted using phenotypic information for earlier time points for known and
458 unknown lines. TP

459 **Acknowledgements**

460 Funding for this research was provided by the National Science Foundation (United States)
461 through Award No. 1238125 to Harkamal Walia.

Table 1: Random regression model selection. Each of the four random regression models included a fixed second-order polynomial to model the mean trend in PSA over the twenty time points, indicated by the column f . G refers to the random additive genetic effect, E the random experimental effect, and e error term. Models with $Diag$ assumed heterogeneous residual variance over time points, while those with I assumed the residual variance was constant. pol^n refers to a Legendre polynomial of order n .

<i>Model</i>	<i>f</i>	<i>G</i>	<i>Exp</i>	<i>e</i>	<i>LogREML</i>	<i>AIC</i>	<i>BIC</i>
Model 1	pol^2	pol^0	pol^0	I	2026.97	-4047.93	-4023.65
Model 2	pol^2	pol^0	pol^0	$Diag$	19358.83	-38673.65	-38495.60
Model 3	pol^2	pol^1	pol^0	I	7345.85	-14681.69	-14641.23
Model 4	pol^2	pol^1	pol^0	$Diag$	23273.62	-46499.24	-46305.01
Model 5	pol^2	pol^2	pol^0	I	8204.64	-16393.28	-16328.54
Model 6	pol^2	pol^2	pol^0	$Diag$	24718.93	-49383.86	-49165.35
Model 7	pol^2	pol^2	pol^0	I	12700.64	-25381.28	-25300.35
Model 8	pol^2	pol^2	pol^1	$Diag$	27537.59	-55017.19	-54782.49

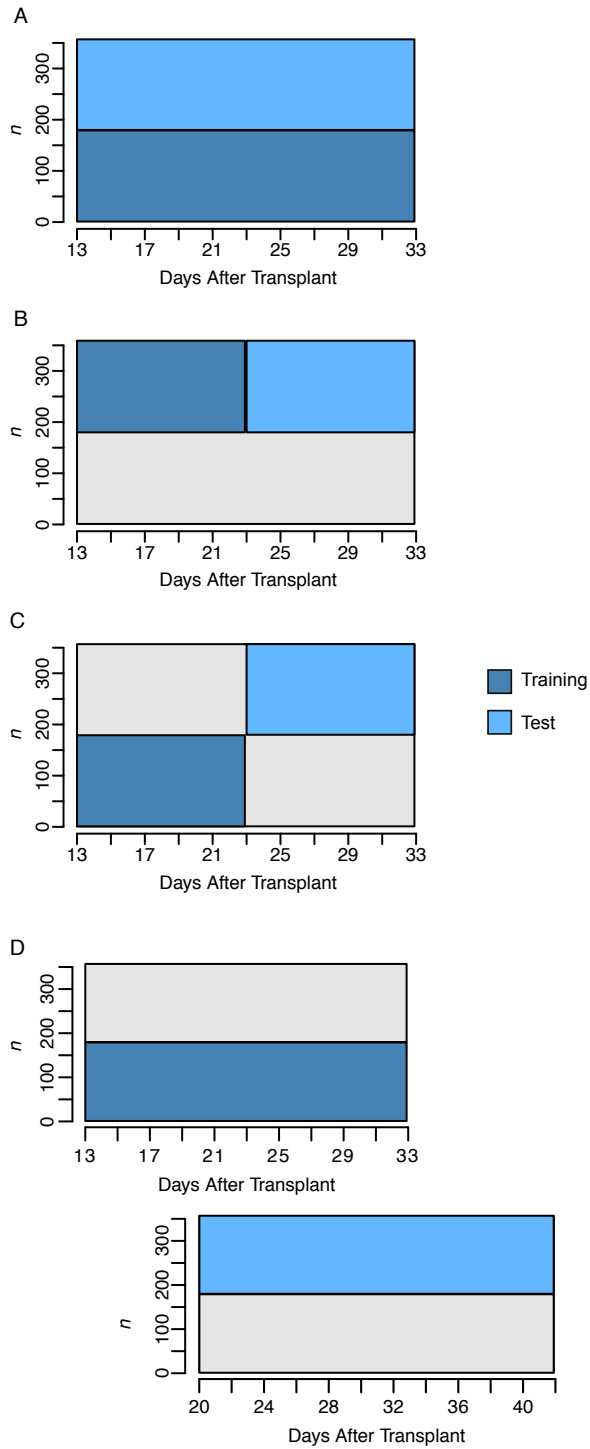


Figure 1: Graphic representation of cross validation schemes for predicting longitudinal phenotypes using random regression. In (A), (C), and (D) two-fold cross validation was

(continued on next page)

used, where phenotypes for 179 lines were used as a training set to predict phenotypes for the remaining 178 lines. In (A), all twenty time points for the training set were used to predict the phenotypes at each of the twenty time points for an new set of lines. The second scenario (B) can be thought of as a forecasting approach where the dataset was split into two longitudinal datasets each consisting of ten time points. The first ten time points for 179 lines and were used to predict the phenotypes at the last ten time points for the same 179 lines. In (C), a forecasting approach was again used, however the lines were randomly split in two, and the first ten time points were used to predict phenotypes in the last ten time points for a group of new lines. In (D) the first 20 time points was used to predict gBLUPs at a later time points in an independent study. Here, a publicly available dataset was used in which 357 lines were phenotyped from 20 to 40 days after transplant, thus a 13 day overlap was available for the two datasets.

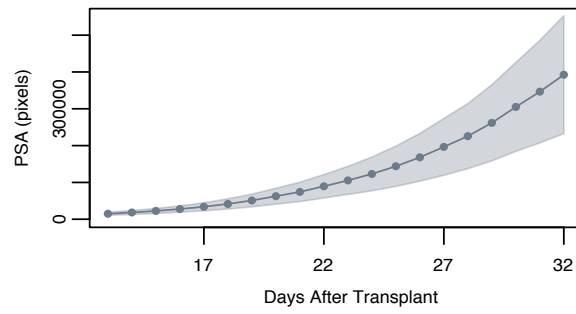


Figure 2: Mean projected shoot area (PSA) across twenty days of imaging. Here, PSA is defined as the sum of plant pixel from three images (two side-view images and one top-view). The shaded region represents the standard deviation of PSA at each time point.

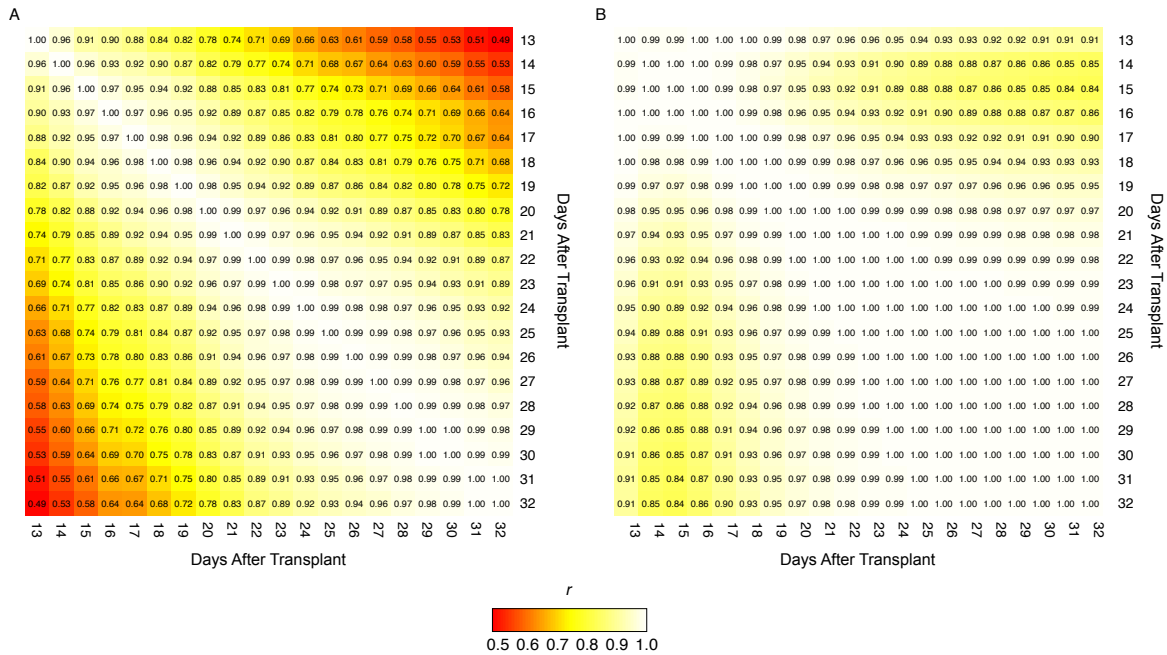


Figure 3: Phenotypic and genetic correlations between each time point. (A) Phenotypic correlations were estimated between time points using Pearson's method. (B) The inferred genetic correlation matrix of random regression terms for the additive genetic effects were used to estimate the genetic correlations between time points. The scale on the left of each panel indicates the strength of the correlations (r).

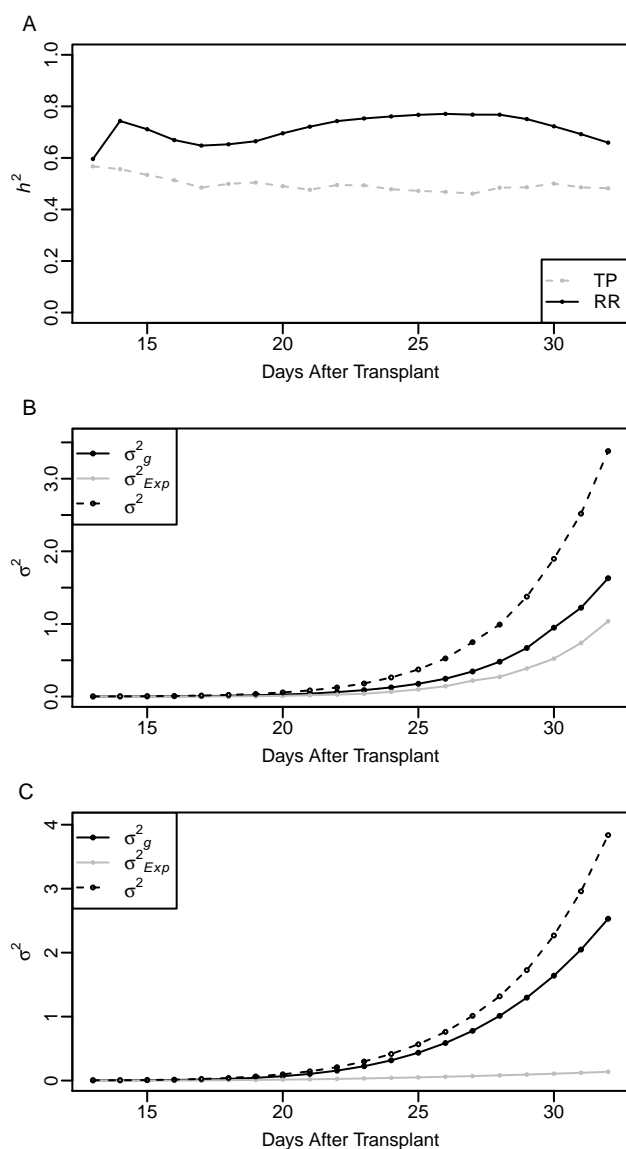


Figure 4: Narrow sense heritability and variance components estimated using the single time point (TP) and random regression (RR) approaches. The narrow sense heritability (h^2) is presented in panel A. Variance components for the TP and RR approaches are pictured in panels B and C, respectively. For the single time point analysis, a conventional mixed model was used to estimate the narrow sense heritability of PSA at each time point. The TP model included a random additive genetic effect and experimental effect. The RR model included a fixed second-order Legendre polynomial, the random additive genetic effect were modeled using a second-order Legendre polynomial, a first-order random effect was used for experiment, and the residual variance was assumed to be heterogeneous over time points. For both models, the experimental term was considered as an environmental effect.

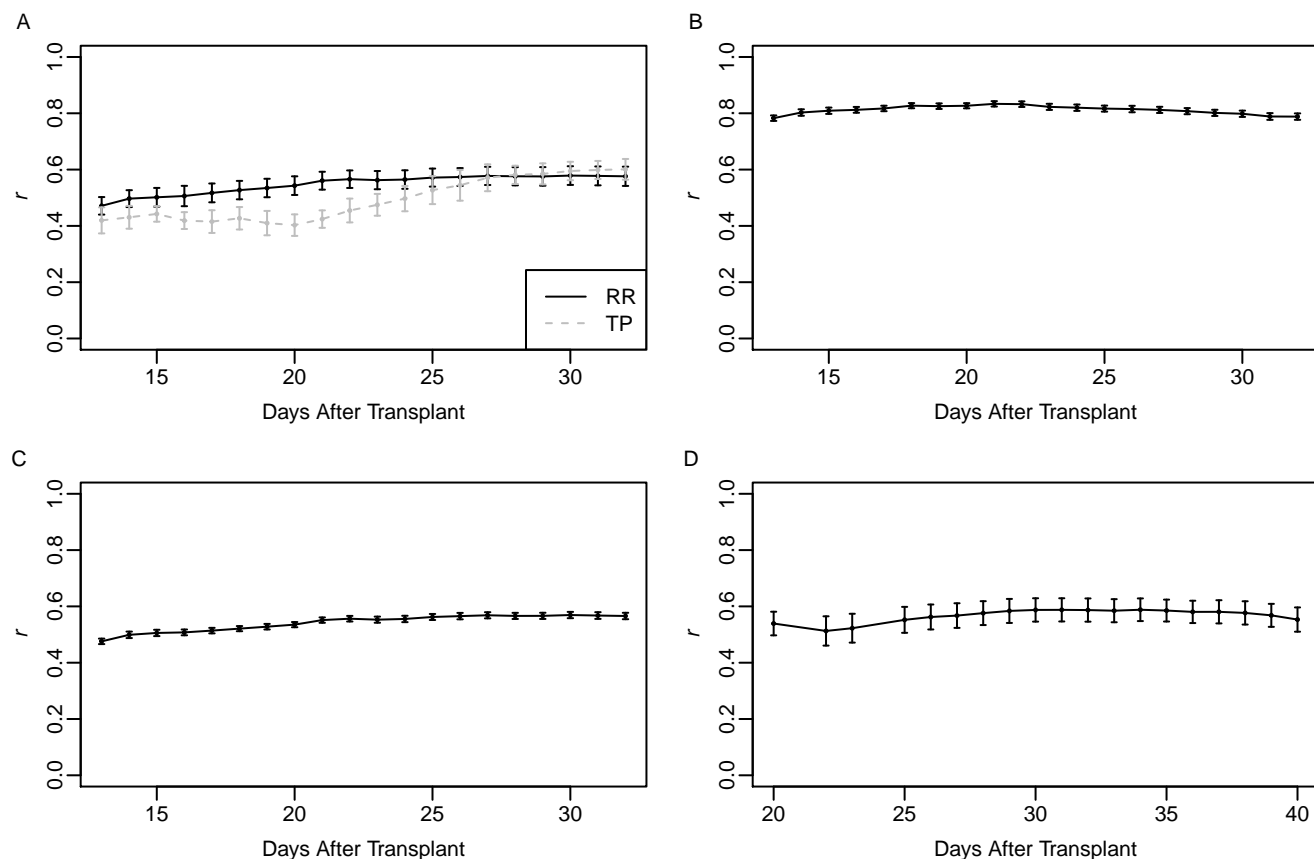


Figure 5: Prediction accuracies of scenarios A to D. For the random regression (RR) approach, a RR model was fit using phenotypic records for 178-179 lines over 20 days. A univariate single time point (TP) run using phenotypic records for 178-179 lines at each day. In both cases, genetic effects from each model were used to predict gBLUPs for the remaining 178-179 lines. Prediction accuracy was assessed using Pearson's correlation between the predicted gBLUPs and observed PSA for the test set. Resampling was done twenty times. The error bars represent the standard deviation where $n = 20$. A comparison of prediction accuracies for TP and RR approaches is presented in (A). Panels B and C present the prediction accuracies for forecasting future phenotypes using phenotypic information at early time points for known lines (B) and new lines (C). Panel D provides prediction accuracies for forecasting future phenotypes in an independent study using phenotypes from an earlier developmental period.

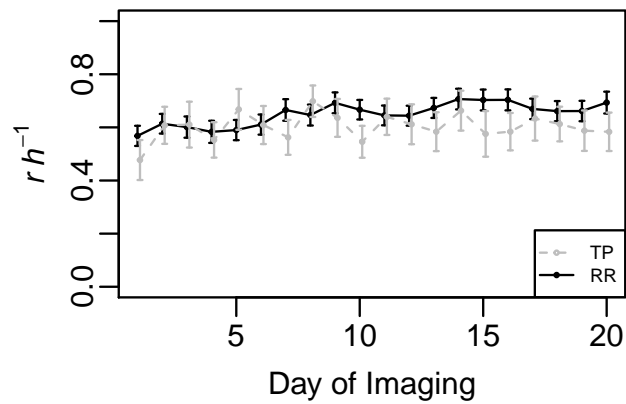


Figure 6: Predictive ability of the random regression (RR) and single time point (TP) approaches expressed as a function of heritability: The analysis followed the same approach as that for scenario A, however for each fold the correlation between gBLUP and observed PSA was divided by the square root of heritability.

References

- 464 Akaike, H., 1974: A new look at the statistical model identification. *IEEE Transactions on*
465 *Automatic Control*, **19 (6)**, 716–723.
- 467 Apiolaza, L. A., A. R. Gilmour, and D. J. Garrick, 2000: Variance modelling of longitudinal
468 height data from a *Pinus radiata* progeny test. *Canadian Journal of Forest Research*,
469 **30 (4)**, 645–654.
- 470 Arruda, M. P., P. J. Brown, A. E. Lipka, A. M. Krill, C. Thurber, and F. L. Kolb, 2015:
471 Genomic selection for predicting fusarium head blight resistance in a wheat breeding pro-
472 gram. *The Plant Genome*, **8 (3)**.
- 473 Berger, B., B. Parent, and M. Tester, 2010: High-throughput shoot imaging to study drought
474 responses. *Journal of Experimental Botany*, **61 (13)**, 3519–3528.
- 475 Bermejo, J. L., R. Roehe, V. Schulze, G. Rave, H. Looft, and E. Kalm, 2003: Random
476 regression to model genetically the longitudinal data of daily feed intake in growing pigs.
477 *Livestock Production Science*, **82 (2)**, 189–199.
- 478 Bohmanova, J., F. Miglior, J. Jamrozik, I. Misztal, and P. Sullivan, 2008: Comparison of
479 random regression models with legendre polynomials and linear splines for production
480 traits and somatic cell score of Canadian Holstein cows. *Journal of Dairy Science*, **91 (9)**,
481 3627–3638.
- 482 Campbell, M. T., Q. Du, K. Liu, C. J. Brien, B. Berger, C. Zhang, and H. Walia, 2017: A
483 comprehensive image-based phenomic analysis reveals the complex genetic architecture of
484 shoot growth dynamics in rice. *The Plant Genome*, **10 (2)**.
- 485 Campbell, M. T., A. C. Knecht, B. Berger, C. J. Brien, D. Wang, and H. Walia, 2015: Inte-

486 grating image-based phenomics and association analysis to dissect the genetic architecture
487 of temporal salinity responses in rice. *Plant Physiology*, **168** (4), 1476–1489.

488 Chapman, S. C., and Coauthors, 2014: Pheno-copter: a low-altitude, autonomous remote-
489 sensing robotic helicopter for high-throughput field-based phenotyping. *Agronomy*, **4** (2),
490 279–301.

491 Costa, C. N., C. M. R. d. Melo, I. U. Packer, A. F. d. Freitas, N. M. Teixeira, and J. A. Cobuci,
492 2008: Genetic parameters for test day milk yield of first lactation Holstein cows estimated
493 by random regression using Legendre polynomials. *Revista Brasileira de Zootecnia*, **37** (4),
494 602–608.

495 Daetwyler, H. D., R. Pong-Wong, B. Villanueva, and J. A. Woolliams, 2010: The impact of
496 genetic architecture on genome-wide evaluation methods. *Genetics*, **185** (3), 1021–1031.

497 Daetwyler, H. D., B. Villanueva, and J. A. Woolliams, 2008: Accuracy of predicting the
498 genetic risk of disease using a genome-wide approach. *PloS One*, **3** (10), e3395.

499 Duhnen, A., A. Gras, S. Teyssèdre, M. Romestant, B. Claustres, J. Daydé, and B. Mangin,
500 2017: Genomic selection for yield and seed protein content in soybean: A study of breeding
501 program data and assessment of prediction accuracy. *Crop Science*, **57** (3), 1325–1337.

502 Endelman, J. B., 2011: Ridge regression and other kernels for genomic selection with R
503 package rrBLUP. *The Plant Genome*, **4** (3), 250–255.

504 Fahlgren, N., M. A. Gehan, and I. Baxter, 2015: Lights, camera, action: high-throughput
505 plant phenotyping is ready for a close-up. *Current Opinion in Plant Biology*, **24**, 93–99.

506 Furbank, R. T., and M. Tester, 2011: Phenomics–technologies to relieve the phenotyping
507 bottleneck. *Trends in Plant Science*, **16** (12), 635–644.

508 Gilmour, A., B. Gogel, B. Cullis, S. Welham, and R. Thompson, 2015: Asreml user guide
509 release 4.1 structural specification. *Hemel Hempstead: VSN International Ltd.*

510 Golzarian, M. R., R. A. Frick, K. Rajendran, B. Berger, S. Roy, M. Tester, and D. S. Lun,
511 2011: Accurate inference of shoot biomass from high-throughput images of cereal plants.
512 *Plant Methods*, **7** (1), 2.

513 Hayes, B. J., P. J. Bowman, A. C. Chamberlain, K. Verbyla, and M. E. Goddard, 2009:
514 Accuracy of genomic breeding values in multi-breed dairy cattle populations. *Genetics*
515 *Selection Evolution*, **41** (1), 51.

516 Howard, J. T., S. Jiao, F. Tiezzi, Y. Huang, K. A. Gray, and C. Maltecca, 2015: Genome-
517 wide association study on Legendre random regression coefficients for the growth and feed
518 intake trajectory on Duroc Boars. *BMC Genetics*, **16** (1), 59.

519 Jannink, J.-L., A. J. Lorenz, and H. Iwata, 2010: Genomic selection in plant breeding: from
520 theory to practice. *Briefings in Functional Genomics*, **9** (2), 166–177.

521 Kirkpatrick, M., D. Lofsvold, and M. Bulmer, 1990: Analysis of the inheritance, selection
522 and evolution of growth trajectories. *Genetics*, **124** (4), 979–993.

523 Knecht, A. C., M. T. Campbell, A. Caprez, D. R. Swanson, and H. Walia, 2016: Image
524 Harvest: an open-source platform for high-throughput plant image processing and analysis.
525 *Journal of Experimental Botany*, **67** (11), 3587–3599.

526 Kristensen, P. S., A. Jahoor, J. R. Andersen, F. Cericola, J. Orabi, L. Janss, and J. Jensen,
527 2018: Genome-wide association studies and comparison of models and cross-validation
528 strategies for genomic prediction of quality traits in advanced winter wheat breeding lines.
529 *Frontiers in Plant Science*, **9**, 69.

530 Leplat, F., J. Jensen, and P. Madsen, 2016: Genomic prediction of manganese efficiency in
531 winter barley. *The Plant Genome*, **9** (2).

532 Lorenz, A. J., and Coauthors, 2011: Genomic selection in plant breeding: knowledge and
533 prospects. *Advances in Agronomy*, Vol. 110, Elsevier, 77–123.

534 Meuwissen, M., B. Hayes, and Goddard, 2001: Prediction of total genetic value using
535 genome-wide dense marker maps. *Genetics*, **157** (4), 1819–1829.

536 Meyer, K., 1998: Estimating covariance functions for longitudinal data using a random
537 regression model. *Genetics Selection Evolution*, **30** (3), 221.

538 Moser, G., S. H. Lee, B. J. Hayes, M. E. Goddard, N. R. Wray, and P. M. Visscher,
539 2015: Simultaneous discovery, estimation and prediction analysis of complex traits us-
540 ing a Bayesian mixture model. *PLoS Genetics*, **11** (4), e1004969.

541 Mrode, R. A., 2014: *Linear models for the prediction of animal breeding values*. CABI.

542 Nobre, P., I. Misztal, S. Tsuruta, J. Bertrand, L. Silva, and P. Lopes, 2003: Analyses of
543 growth curves of Nelore cattle by multiple-trait and random regression models. *Journal*
544 *of Animal Science*, **81** (4), 918–926.

545 Rutkoski, J., J. Poland, S. Mondal, E. Autrique, L. G. Pérez, J. Crossa, M. Reynolds,
546 and R. Singh, 2016: Canopy temperature and vegetation indices from high-throughput
547 phenotyping improve accuracy of pedigree and genomic selection for grain yield in wheat.
548 *G3: Genes, Genomes, Genetics*, **6** (9), 2799–2808.

549 Sun, J., J. E. Rutkoski, J. A. Poland, J. Crossa, J.-L. Jannink, and M. E. Sorrells, 2017: Mul-
550 titrait, random regression, or simple repeatability model in high-throughput phenotyping
551 data improve genomic prediction for wheat grain yield. *The Plant Genome*, **10** (2).

- 552 VanRaden, P. M., 2008: Efficient methods to compute genomic predictions. *Journal of Dairy*
553 *Science*, **91 (11)**, 4414–4423.
- 554 Wang, C., B. Andersson, and P. Waldmann, 2009: Genetic analysis of longitudinal height
555 data using random regression. *Canadian Journal of Forest Research*, **39 (10)**, 1939–1948.
- 556 Watanabe, K., and Coauthors, 2017: High-throughput phenotyping of sorghum plant height
557 using an unmanned aerial vehicle and its application to genomic prediction modeling.
558 *Frontiers in Plant Science*, **8**.
- 559 Wetten, M., J. Ødegård, O. Vangen, and T. H. Meuwissen, 2012: Simultaneous estimation of
560 daily weight and feed intake curves for growing pigs by random regression. *Animal*, **6 (3)**,
561 433–439.
- 562 Yu, J., and Coauthors, 2006: A unified mixed-model method for association mapping that
563 accounts for multiple levels of relatedness. *Nature Genetics*, **38 (2)**, 203.
- 564 Zhang, J., C. Yang, H. Song, W. C. Hoffmann, D. Zhang, and G. Zhang, 2016: Evaluation
565 of an airborne remote sensing platform consisting of two consumer-grade cameras for crop
566 identification. *Remote Sensing*, **8 (3)**, 257.
- 567 Zhao, K., and Coauthors, 2011: Genome-wide association mapping reveals a rich genetic
568 architecture of complex traits in *Oryza sativa*. *Nature Communications*, **2**, 467.